

# Cystathionine $\beta$ -Synthase (CBS) Domain-containing Pyrophosphatase as a Target for Diadenosine Polyphosphates in Bacteria\*

Received for publication, July 21, 2015, and in revised form, September 11, 2015. Published, JBC Papers in Press, September 23, 2015, DOI 10.1074/jbc.M115.680272

Viktor A. Anashkin<sup>†‡§</sup>, Anu Salminen<sup>‡</sup>, Heidi K. Tuominen<sup>‡</sup>, Victor N. Orlov<sup>§</sup>, Reijo Lahti<sup>†1</sup>, and Alexander A. Baykov<sup>§2</sup>

From the <sup>‡</sup>Department of Biochemistry, University of Turku, FIN-20014 Turku, Finland and the <sup>§</sup>Belozersky Institute of Physico-Chemical Biology and Department of Chemistry, Lomonosov Moscow State University, Moscow 119899, Russia

**Background:** Many soluble pyrophosphatases contain two regulatory nucleotide-binding CBS domains with or without an intercalating DRTGG domain.

**Results:** Linear P<sup>1</sup>,P<sup>n</sup>-diadenosine 5'-polyphosphates (Ap<sub>n</sub>As, n = 3–6) bind with nanomolar affinity to and activate DRTGG domain-containing pyrophosphatases; Ap<sub>3</sub>A binds cooperatively.

**Conclusion:** Nucleotide-regulated pyrophosphatases may represent receptors for Ap<sub>n</sub>As in bacteria.

**Significance:** The results suggest a novel regulatory pathway in some bacteria, involving Ap<sub>n</sub>As as messengers.

Among numerous proteins containing pairs of regulatory cystathionine  $\beta$ -synthase (CBS) domains, family II pyrophosphatases (CBS-PPases) are unique in that they generally contain an additional DRTGG domain between the CBS domains. Adenine nucleotides bind to the CBS domains in CBS-PPases in a positively cooperative manner, resulting in enzyme inhibition (AMP or ADP) or activation (ATP). Here we show that linear P<sup>1</sup>,P<sup>n</sup>-diadenosine 5'-polyphosphates (Ap<sub>n</sub>As, where n is the number of phosphate residues) bind with nanomolar affinity to DRTGG domain-containing CBS-PPases of *Desulfotobacterium hafniense*, *Clostridium novyi*, and *Clostridium perfringens* and increase their activity up to 30-, 5-, and 7-fold, respectively. Ap<sub>4</sub>A, Ap<sub>5</sub>A, and Ap<sub>6</sub>A bound noncooperatively and with similarly high affinities to CBS-PPases, whereas Ap<sub>3</sub>A bound in a positively cooperative manner and with lower affinity, like mononucleotides. All Ap<sub>n</sub>As abolished kinetic cooperativity (non-Michaelian behavior) of CBS-PPases. The enthalpy change and binding stoichiometry, as determined by isothermal calorimetry, were ~10 kcal/mol nucleotide and 1 mol/mol enzyme dimer for Ap<sub>4</sub>A and Ap<sub>5</sub>A but 5.5 kcal/mol and 2 mol/mol for Ap<sub>3</sub>A, AMP, ADP, and ATP, suggesting different binding modes for the two nucleotide groups. In contrast, *Eggerthella lenta* and *Moorella thermoacetica* CBS-PPases, which contain no DRTGG domain, were not affected by Ap<sub>n</sub>As and showed no enthalpy change, indicating the importance of the DRTGG domain for Ap<sub>n</sub>A binding. These findings suggest that Ap<sub>n</sub>As can control CBS-PPase activity and hence affect pyrophosphate level and biosynthetic activity in bacteria.

Diadenosine polyphosphates (Ap<sub>n</sub>As)<sup>3</sup> are ubiquitous compounds in which two adenosine moieties are linked through ribose 5'-C by a chain of three to six phosphate residues. First discovered in 1965 as by-products of chemical ATP synthesis (1), Ap<sub>n</sub>As have subsequently been identified in organisms belonging to all kingdoms of life. Many enzymatic reactions leading to Ap<sub>n</sub>As are known (2), of which the reaction catalyzed by aminoacyl-tRNA synthetase, lysyl-tRNA synthetase in particular (3), is the best known. *Escherichia coli* lysyl-tRNA synthetase produces Ap<sub>n</sub>As by a side reaction during lysyl-tRNA synthesis via attack of the terminal phosphate group of ATP and other monoadenosine phosphates on the enzyme-bound aminoacyl adenylate intermediate (4). Because ATP prevails in cells, the product of its reaction with aminoacyl adenylate, Ap<sub>4</sub>A, is the most prevalent Ap<sub>n</sub>A. Lysyl-tRNA synthetase can additionally convert Ap<sub>4</sub>A to Ap<sub>3</sub>A (5). Ap<sub>n</sub>As are degraded in the cell by specific and nonspecific enzymes, including Ap<sub>4</sub>A hydrolase and phosphodiesterase (6, 7), which balance the intracellular concentration of Ap<sub>n</sub>As at a submicromolar level. However, their concentrations in prokaryotes can rise up to 300  $\mu$ M under stress conditions (8).

Because of its association with stress, AP<sub>4</sub>A was originally classified as an intracellular “alarmone” (8–10). An alternative view is that AP<sub>4</sub>A formation represents a compensatory mechanism that helps to sustain basic physiology during stress and assist in the return to normal physiology in bacteria (11). In eukaryotes, Ap<sub>n</sub>As may have a second messenger role (12). Regardless of which theory is true, it is clear that Ap<sub>n</sub>As participate, in some as yet poorly understood ways, in a number of cellular phenomena associated with stress, such as DNA replication and repair (13) and cell division (14). In eukaryotes,

\* This work was supported by Academy of Finland Grant 139031 and Russian Foundation for Basic Research Grants 12-04-01002 and 15-04-04828. The authors declare that they have no conflicts of interest with the contents of this article.

<sup>1</sup> To whom correspondence may be addressed: Dept. of Biochemistry, University of Turku, Vatselankatu 2, FIN-20014 Turku, Finland. Tel.: 358-2353-6845; Fax: 358-2353-6860; E-mail: reijo.lahti@utu.fi.

<sup>2</sup> To whom correspondence may be addressed: Dept. of Protein Chemistry, Belozersky Institute of Physico-Chemical Biology, Lomonosov Moscow State University, Moscow 119992, Russia. Tel.: 7-495-939-5541; Fax: 7-495-939-0358; E-mail: baykov@genebee.msu.su.

<sup>3</sup> The abbreviations used are: Ap<sub>n</sub>A, 5',5'-P<sup>1</sup>,P<sup>n</sup>-diadenosine polyphosphate with n phosphate residues; CBS, cystathionine  $\beta$ -synthase; CBS-PPase, CBS domain-containing pyrophosphatase; *cn*PPase, *C. novyi* pyrophosphatase; *cp*PPase, *C. perfringens* pyrophosphatase; *dh*PPase, *D. hafniense* pyrophosphatase; *el*PPase, *E. lenta* pyrophosphatase; *mt*PPase, *M. thermoacetica* pyrophosphatase; PPase, pyrophosphatase; TES, 2-[[2-hydroxy-1,1-bis(hydroxymethyl)ethyl]amino]ethanesulfonic acid; ITC, isothermal titration calorimetry.

Ap<sub>n</sub>As are involved in many other processes, including neurotransmission (15), apoptosis (16), and analgesia (17). Of note, Ap<sub>4</sub>A is used in hypoxia therapy in humans (18).

Understanding the roles of Ap<sub>n</sub>As requires knowledge of their target proteins. Using a radioactive photocrosslinking Ap<sub>4</sub>A analog, Johnstone and Farr (19) detected 12 Ap<sub>4</sub>A-binding proteins in *E. coli* extract, some of which were identified as heat shock proteins based on their electrophoretic mobilities. Guo *et al.* (20) and Azhar *et al.* (21) used pulldown assays with immobilized Ap<sub>4</sub>A analogs followed by mass-spectral analysis to identify, respectively, 6 and 13 binding proteins in *E. coli*. The three protein sets obtained in these studies partially overlapped. Few Ap<sub>n</sub>A protein complexes have been subjected to biophysical and mechanistic studies. Apart from cases where Ap<sub>n</sub>As act as substrates or products of their metabolizing enzymes, the chaperone GroEL binds Ap<sub>4</sub>A with a dissociation constant of 10 μM; the complex exhibits increased ATPase and chaperoning activities (11). Human 5'-nucleotidase II is allosterically activated by Ap<sub>n</sub>As ( $n = 4-6$ ), which bind with dissociation constants of 60–80 μM (22).

Inorganic pyrophosphatases (PPases; EC 3.6.1.1), the major PP<sub>i</sub>-metabolizing enzymes in all types of organisms, belong to three nonhomologous families (23). Family II PPases, found in bacteria and archaea, are homodimeric Mn<sup>2+</sup>- or Co<sup>2+</sup>-metalloenzymes that additionally require Mg<sup>2+</sup> for catalysis (24). A quarter of the more than 500 putative family II PPase sequences contain a regulatory insert comprising a pair of cystathionine β-synthase (CBS) domains (Bateman module (25)) within one of the two catalytic domains. Regulatory CBS domains are found in proteins in all kingdoms of life and generally bind adenine nucleotides as regulating molecules (26–28); mutations in CBS domains of human proteins are associated with hereditary diseases (29, 30). Interestingly, only in CBS-PPases (but not all of them), are the CBS domains intercalated by another (DRTGG) domain. CBS-PPases are activated by ATP and inhibited by AMP and ADP (31, 32). Both catalysis and regulation involve marked positive cooperativity, which is Mg<sup>2+</sup>-dependent (32).

The structure of the isolated dimeric regulatory insert of *Clostridium perfringens* PPase (*cp*PPase) obtained for crystals grown in the presence of 0.25 mM Ap<sub>4</sub>A contains an Ap<sub>4</sub>A molecule bound by two CBS domain pairs at the subunit interface (33), raising the possibility that Ap<sub>4</sub>A may be a physiological ligand of CBS-PPases. Preliminary activity measurements (33, 34) suggested that Ap<sub>4</sub>A activates *cp*PPase. Here we show that all Ap<sub>n</sub>As bind with nanomolar affinities to three DRTGG domain-containing CBS-PPases and modulate their catalytic activity and cooperative behavior. Our data thus identify a new type of ligand for CBS domains and an important target of Ap<sub>n</sub>As in the protein world.

## Experimental Procedures

**Enzymes and Reagents**—Genes for CBS-PPases from *Desulfitobacterium hafniense* (*dh*PPase), *Clostridium novyi* (*cn*PPase), *C. perfringens* (*cp*PPase), *Eggerthella lenta* (*el*PPase), and *Moorella thermoacetica* (*mt*PPase) were expressed in *E. coli*, and the produced CBS-PPases were purified as described previously (32–34). Inactive aggregates were sepa-

rated from soluble active proteins during size exclusion chromatography. The final products were at least 95% pure as estimated by SDS-PAGE using a Phast system with 8–25% gradient gels (GE Healthcare). Protein concentrations were determined with a Nanodrop spectrophotometer (Thermo Scientific) using  $A_{280}^{0.1\%}$  of 0.478 for *dh*PPase, 0.548 for *cn*PPase, 0.426 for *cp*PPase, 0.493 for *el*PPase, and 0.48 for *mt*PPase, as calculated from their amino acid compositions with ProtParam. Molar concentrations were calculated based on subunit molecular masses of 60.4, 63.6, 60.8, 52.5, and 48.1 kDa, respectively. All enzyme concentrations are given in terms of the dimer.

P<sup>1</sup>,P<sup>n</sup>-diadenosine 5'-polyphosphates (Ap<sub>n</sub>As) with  $n = 3-5$  were from Sigma; Ap<sub>6</sub>A was from Jena Bioscience. All Ap<sub>n</sub>As were ≥97% pure, and Ap<sub>3</sub>A was essentially free of other Ap<sub>n</sub>As, according to the manufacturer analyses (HPLC). The concentrations of stock nucleotide solutions were calibrated by measuring absorbance in the ultraviolet region ( $\epsilon_{259} = 31,800 \text{ M}^{-1}\text{cm}^{-1}$  for dinucleotides and  $15,900 \text{ M}^{-1}\text{cm}^{-1}$  for mononucleotides).

**Kinetic Assays**—The activity assay medium contained 5 mM MgCl<sub>2</sub>, 140 μM PP<sub>i</sub> (yielding 50 μM MgPP<sub>i</sub> complex) and 0.1 M TES-KOH (pH 7.2), except where specified otherwise. In measurements done at higher Mg<sup>2+</sup> concentrations, buffer concentration was decreased appropriately to maintain constant ionic strength. The reaction was initiated by adding enzyme, and P<sub>i</sub> accumulation caused by PP<sub>i</sub> hydrolysis was continuously recorded for 2–3 min at 25 °C using an automated P<sub>i</sub> analyzer (35). Initial velocities of PP<sub>i</sub> hydrolysis were typically estimated graphically from the slopes of the tangents to the initial portion of hydrolysis time courses recorded with the P<sub>i</sub> analyzer.

**Isothermal Calorimetry**—A VP-iTC calorimeter (MicroCal Ltd.) was used. Enzyme and nucleotide solutions were made in 0.1 M MOPS/KOH (pH 7.2) buffer containing 2 mM MgCl<sub>2</sub>, 0.1 mM CoCl<sub>2</sub>, and 150 mM KCl. Titrations were performed at 25 °C by successive 10-μl injections of 0.1–10 mM mononucleotide or 33 μM dinucleotide solution into 2 ml of CBS-PPase solution (2.5–5 μM in terms of the dimer); the interval between injections was 5 min. All samples were degassed before the experiment. Binding isotherms were corrected by subtracting the ligand dilution isotherms, determined by titrating nucleotide solutions into the buffer.

**Calculations and Data Analysis**—The values of the apparent dissociation constants for the magnesium complexes of PP<sub>i</sub> used to maintain required free Mg<sup>2+</sup> ion and MgPP<sub>i</sub> complex concentrations at pH 7.2 were 112 μM for MgPP<sub>i</sub> and 2.84 mM for Mg<sub>2</sub>PP<sub>i</sub> (36). Nonlinear least square fittings were performed using the program Scientist (Micromath). The dependence of hydrolysis rate on nucleotide concentration ([N]) was fit to Equation 1,

$$v = \{v_N + (v_0 + v_N)K_{N2}/2[N] + v_0K_{N1}K_{N2}/[N]^2\}/(1 + K_{N2}/[N] + K_{N1}K_{N2}/[N]^2) \quad (\text{Eq. 1})$$

where  $v_0$  and  $v_N$  are activities of free and nucleotide-saturated enzyme, respectively, and  $K_{N1}$  and  $K_{N2}$  are the macroscopic dissociation constants describing successive binding of nucleotide to two regulatory sites per enzyme molecule. Cooperative kinetics of substrate (MgPP<sub>i</sub>) hydrolysis were analyzed with Equation 2,

## Nucleotide-regulated Soluble Pyrophosphatases

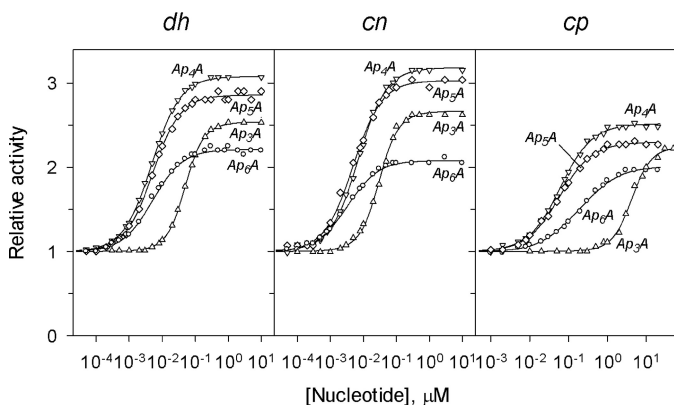


**FIGURE 1. Concentration dependences of the effects of  $Ap_n$ As on the activity of three CBS-PPases measured at fixed concentrations of substrate ( $50 \mu\text{M MgPP}_i$ ) and  $\text{Mg}^{2+}$  ( $5 \text{ mM}$ ).** The lines show the best fits of Equations 1 or 4 (see text for details). Activity without nucleotides ( $220$ ,  $350$ , and  $800 \text{ s}^{-1}$  for  $dh$ PPase,  $cn$ PPase and  $cp$ PPase, respectively) was taken as unity.  $dh$ ,  $dh$ PPase;  $cn$ ,  $cn$ PPase;  $cp$ ,  $cp$ PPase.

$$v = k_{\text{cat}}[E]_0(1 + 0.5K_{m2}/[S]) / (1 + K_{m2}/[S] + K_{m1}K_{m2}/[S]^2) \quad (\text{Eq. 2})$$

which assumes different Michaelis constants ( $K_{m1}$  and  $K_{m2}$ ) and equal  $k_{\text{cat}}$  values for the two active sites in the dimer.  $[E]_0$  and  $[S]$  are total enzyme and substrate concentrations, respectively. The corresponding binding schemes and details of the fitting procedure were described previously (32).

The dependences of  $K_{N1}$ ,  $K_{N2}$ ,  $K_{m1}$ , and  $K_{m2}$  on  $\text{Mg}^{2+}$  ( $M$ ) concentration were fit to Equation 3,

$$K_L = (K_L)_0(1 + [M]/K_M) / \{1 + (K_L)_0[M]/(K_L)_M K_M\} \quad (\text{Eq. 3})$$

where  $(K_L)_0$  and  $(K_L)_M$  are the limiting values of the respective  $K_N$  or  $K_m$  at 0 and infinite  $\text{Mg}^{2+}$  concentrations, and  $K_M$  is the metal binding constant.

Alternatively, rate dependences on substrate and nucleotide concentrations were fit to a Hill-type Equation 4,

$$v = v_0 + (v_L - v_0) / (1 + K_L/[L]^h) \quad (\text{Eq. 4})$$

where  $L$  is  $S$  or  $N$ ,  $v_L$  is the rate at infinite  $[L]$ , and  $h$  is the Hill coefficient. The value of  $v_0$  was set to 0 when  $L$  was substrate, and the value of  $h$  was set to unity for noncooperative binding.

Isothermal titration calorimetry (ITC) data were analyzed with a MicroCal ITC subroutine in Origin 7.0 software using a single-binding site model. Thermodynamic parameters were calculated from the standard relationship,  $\Delta G = RT \ln K_N = \Delta H - T\Delta S$ .

### Results

**Effects of  $Ap_n$ As on CBS-PPases at a Fixed  $\text{Mg}^{2+}$  Concentration**—Fig. 1 shows the concentration dependences of the effects of four  $Ap_n$ As with  $n = 3-6$  on the activities of three CBS-PPases measured at fixed substrate ( $\text{MgPP}_i$ ) and  $\text{Mg}^{2+}$  concentrations ( $50 \mu\text{M}$  and  $5 \text{ mM}$ , respectively). Nanomolar concentrations of  $Ap_n$ As caused marked activation in all cases, except that  $Ap_3A$  was effective with  $cp$ PPase at micromolar concentrations.

Analyses of the dependences shown in Fig. 1 and of similar dependences measured at different substrate concentrations (1

and  $300 \mu\text{M}$ ) were initially done using Equation 4. The value of the Hill coefficient was indistinguishable from unity ( $1 \pm 0.05$ ) at all substrate concentrations for  $Ap_n$ As with  $n = 4-6$ . In contrast,  $Ap_3A$  bound cooperatively ( $h = 1.4-1.7$ ) at all substrate concentrations. Accordingly, the data for  $Ap_3A$  were analyzed with Equations 1 and 4 in their general forms, whereas Equation 4 with  $h = 1$  was used for the other  $Ap_n$ As. The parameter values derived from this analysis are summarized in Tables 1 and 2.

The values of the activation factor ( $v_N/v_0$ ) and their trends with changing polyphosphate length and substrate concentration were similar for the three enzymes. The value of  $v_N/v_0$  was greater at low than at high substrate concentrations. In the presence of  $300 \mu\text{M}$  substrate, which is in excess of the respective Michaelis constants (32),  $v_N/v_0$  approached a value of  $\sim 2$  in all cases.

The apparent binding affinities of the nucleotides could be compared on the basis of the average binding constant ( $\sqrt{K_{N1}K_{N2}}$ ) for  $Ap_3A$  and respective  $K_N$  values for the other dinucleotides. As Tables 1 and 2 make clear, the binding affinity estimated at  $50 \mu\text{M}$  substrate was markedly lower for  $Ap_3A$  compared with other dinucleotides for all CBS-PPases. Increasing  $n$  did not affect  $dh$ PPase affinity, but it did slightly increase  $cn$ PPase affinity and decrease  $cp$ PPase affinity. Increasing substrate concentration had opposite effects on the affinity of  $Ap_3A$  and  $Ap_4A$  for  $dh$ PPase and  $cp$ PPase (increased) and  $cn$ PPase (decreased). Of note,  $cp$ PPase exhibited much lower affinity for all dinucleotides compared with other CBS-PPases.

Surprisingly, neither dinucleotide at a concentration up to  $10 \mu\text{M}$  affected activities of  $el$ PPase or  $mt$ PPase measured with  $50 \mu\text{M}$  substrate. These CBS-PPases differ from those described above by having no DRTGG domain in their regulatory regions, which are formed by only two CBS domains. Moreover,  $10 \mu\text{M}$   $Ap_4A$  did not affect the concentration dependence of ADP inhibition of  $el$ PPase or  $mt$ PPase (data not shown), indicating that the dinucleotide is unable to interact with the ADP-binding site.

**Dependence of CBS-PPase Activation on  $\text{Mg}^{2+}$  Concentration**—Given that cooperativity in CBS-PPases is  $\text{Mg}^{2+}$ -dependent (32), measurements analogous to those illustrated in Fig. 1 were conducted for two representative dinucleotides,  $Ap_3A$  and  $Ap_4A$ , over a  $0.05-20 \text{ mM}$   $\text{Mg}^{2+}$  concentration range; substrate concentration was fixed at  $50 \mu\text{M}$ . The results of these experiments (Fig. 2) indicated that  $Ap_3A$  bound with positive cooperativity and  $Ap_4A$  bound noncooperatively to all CBS-PPases at all  $\text{Mg}^{2+}$  concentrations. In only one case ( $dh$ PPase with  $Ap_3A$ ), the degree of cooperativity, as characterized by the values of  $h$  and the ratio  $K_{N2}/K_{N1}$ , showed a pronounced dependence on  $[\text{Mg}^{2+}]$  because of the opposite effects of  $\text{Mg}^{2+}$  on  $K_{N1}$  and  $K_{N2}$  (Fig. 2). In all other cases,  $K_{N1}$  and  $K_{N2}$  changed in the same direction to approximately the same degree and, consequently, without a marked effect on cooperativity. Of note, the ratio  $K_{N2}/K_{N1}$  equals 4 in the case of noncooperative binding and is less than 4 for positively cooperative binding (37).

In most cases (except for  $dh$ PPase with  $Ap_4A$ ),  $\text{Mg}^{2+}$  modulated dinucleotide binding, with the direction of the effect depending on both the nature of the nucleotide and the CBS-

**TABLE 1**  
Kinetic parameters for activation of three CBS-PPases by Ap<sub>3</sub>A in the presence of 5 mM Mg<sup>2+</sup>

Enzyme	[MgPP <sub>i</sub> ] μM	v <sub>N</sub> /v <sub>0</sub> <sup>a</sup>	K <sub>N1</sub>	K <sub>N2</sub>	$\sqrt{K_{N1}K_{N2}}$	4K <sub>N1</sub> /K <sub>N2</sub>	<i>h</i>
<i>dh</i> PPase	1	32 ± 6	460 ± 80	100 ± 20	213 ± 5	18 ± 7	1.60 ± 0.05
	50	2.54 ± 0.01	82 ± 6	30 ± 2	50.0 ± 0.4	10.8 ± 1.4	1.51 ± 0.02
	300	1.78 ± 0.03	12 ± 4	4 ± 1	7.1 ± 0.4	12 ± 8	1.50 ± 0.10
<i>cn</i> PPase	1	5.1 ± 0.1	19 ± 1	12 ± 1	14.8 ± 0.3	7 ± 1	1.42 ± 0.04
	50	2.67 ± 0.05	41 ± 8	22 ± 4	30 ± 1	7 ± 3	1.43 ± 0.07
	300	1.77 ± 0.01	55 ± 9	22 ± 4	35.2 ± 0.9	6.3 ± 1.6	1.40 ± 0.04
<i>cp</i> PPase	1	6.8 ± 0.1	26,000 ± 4,000	3,400 ± 600	9,000 ± 300	31 ± 10	1.66 ± 0.06
	50	2.25 ± 0.05	12,000 ± 5,000	1,500 ± 700	4,200 ± 200	31 ± 29	1.69 ± 0.12
	300	2.24 ± 0.02	1,800 ± 0.2	700 ± 100	1,130 ± 30	10 ± 3	1.50 ± 0.05

<sup>a</sup> v<sub>N</sub> and v<sub>0</sub> are activities extrapolated to infinite concentration of the variable nucleotide and measured in the absence of any nucleotide, respectively.

**TABLE 2**  
Kinetic parameters for activation of three CBS-PPases by diadenosine polyphosphates with *n* = 4–6 in the presence of 5 mM Mg<sup>2+</sup>

The value of the Hill coefficient was indistinguishable from unity in all cases.

Enzyme/dinucleotide	[MgPP <sub>i</sub> ] μM	v <sub>N</sub> /v <sub>0</sub> <sup>a</sup>	K <sub>N</sub> <sup>b</sup>
<i>dh</i> PPase Ap <sub>4</sub> A	1	18 ± 1	12.1 ± 0.3
	50	3.0 ± 0.1	4.9 ± 0.2
	300	1.91 ± 0.02	4.3 ± 0.2
	50	3.32 ± 0.06	5.5 ± 0.2
<i>cn</i> PPase Ap <sub>4</sub> A	1	6.0 ± 0.3	3.9 ± 0.1
	50	3.14 ± 0.05	7.0 ± 0.2
	300	1.51 ± 0.01	16.5 ± 0.7
	50	3.03 ± 0.08	4.9 ± 0.3
<i>cp</i> PPase Ap <sub>4</sub> A	1	14.7 ± 0.4	293 ± 5
	50	2.52 ± 0.03	62 ± 2
	300	2.04 ± 0.02	33 ± 1
	50	2.30 ± 0.03	58 ± 2
Ap <sub>5</sub> A	50	2.30 ± 0.03	58 ± 2
	50	2.04 ± 0.02	187 ± 9

<sup>a</sup> v<sub>N</sub> and v<sub>0</sub> are activities extrapolated to infinite concentration of the variable nucleotide and measured in the absence of any nucleotide, respectively.

<sup>b</sup> This parameter is equivalent to  $\sqrt{K_{N1}K_{N2}}$  in Table 1.

PPase origin (Figs. 2 and 3). Mg<sup>2+</sup> generally stimulated Ap<sub>3</sub>A binding, except for *dh*PPase, where it exerted the opposite effect on K<sub>N1</sub> (Fig. 2). Mg<sup>2+</sup> exhibited a full range of effects on Ap<sub>4</sub>A binding (Fig. 2): stimulation (*cp*PPase), suppression (*cn*PPase), and no effect (*dh*PPase). The effect of Mg<sup>2+</sup> on dinucleotide binding could be described by Equation 3, yielding the parameter values summarized in Table 3. The values of K<sub>m</sub> governing the Mg<sup>2+</sup> effects were in the millimolar range and were similar for both steps of Ap<sub>3</sub>A binding and Ap<sub>4</sub>A binding for a given CBS-PPase.

The degree of activation (v<sub>N</sub>/v<sub>0</sub>) of *dh*PPase and *cn*PPase by Ap<sub>3</sub>A and Ap<sub>4</sub>A demonstrated no or only small variations with Mg<sup>2+</sup> concentration (Fig. 2). In contrast, activation of *cp*PPase showed a bell-shaped dependence (Ap<sub>3</sub>A) or markedly decreased (Ap<sub>4</sub>A) with increasing Mg<sup>2+</sup> concentration.

**Analysis of CBS-PPase Activation in Terms of Michaelis-Menten Parameters**—As previously reported, the rate of MgPP<sub>i</sub> hydrolysis by CBS-PPases does not obey Michaelis-Menten kinetics, requiring the use of a more complex equation with two Michaelis constants (32). Their ratio, K<sub>m2</sub>/K<sub>m1</sub>, was less than 4, and the Hill coefficient was greater than 1, indicating positive kinetic cooperativity.

Surprisingly, Ap<sub>3</sub>A and Ap<sub>4</sub>A completely abolished or markedly suppressed the kinetic cooperativity in *dh*PPase, *cn*PPase

and *cp*PPase, as indicated by a Hill coefficient with a value close to 1 (Table 4 and Fig. 3). That the *h* value is greater than 1 for *cp*PPase in the presence of Ap<sub>3</sub>A may reflect incomplete saturation of this enzyme by the dinucleotide, which binds much more weakly to *cp*PPase compared with the other CBS-PPases, especially at low substrate concentrations (Table 1).

The kinetics of activation by Ap<sub>4</sub>A was investigated over a range of Mg<sup>2+</sup> concentrations (Fig. 3). The results showed that 10 μM activator increased k<sub>cat</sub>, decreased the Michaelis constant, and abolished kinetic cooperativity. Again the largest effects were observed with *cp*PPase, which was therefore explored in greater detail.

The effects of four Ap<sub>n</sub>As on the Mg<sup>2+</sup> concentration dependence of k<sub>cat</sub> for *cp*PPase were qualitatively similar (Fig. 4). Mg<sup>2+</sup> induced a transition from low to high activity over a narrow range of concentrations, requiring a term with [Mg<sup>2+</sup>]<sup>2</sup> in the corresponding equation (see Fig. 3 legend) (32). All four activators increased the limiting value of k<sub>cat</sub> at infinite [Mg<sup>2+</sup>] (k<sub>cat,M</sub>) and decreased the Mg<sup>2+</sup> binding constant (K<sub>m</sub>) ~2-fold (Table 5). Most surprisingly, Ap<sub>n</sub>A binding conferred catalytic activity to the otherwise inactive *cp*PPase at low [Mg<sup>2+</sup>] (see k<sub>cat,0</sub> values in Table 5). The activity of Ap<sub>4</sub>A-activated *cp*PPase in these conditions approached its maximum activity observed at high [Mg<sup>2+</sup>] in the absence of Ap<sub>4</sub>A (Fig. 4).

Fig. 5 illustrates the concentration dependence of *cp*PPase activation by Ap<sub>4</sub>A in the presence of 0.5 mM Mg<sup>2+</sup>, analyzed in terms of k<sub>cat</sub> and K<sub>m</sub> values. The value of k<sub>cat</sub> increased ~7.5-fold (from 240 ± 100 to 1800 ± 100 s<sup>-1</sup>), K<sub>m1</sub> decreased ~18-fold (from 70 ± 10 to 4 ± 1 μM), and K<sub>m2</sub> changed insignificantly with increasing Ap<sub>4</sub>A concentration from 0 to 5 μM. The Ap<sub>4</sub>A binding constant estimated from k<sub>cat</sub> and K<sub>m1</sub> dependences was 0.04 ± 0.01 and 1.7 ± 1.0 μM, respectively. Because k<sub>cat</sub> and K<sub>m</sub> dependences report on Ap<sub>4</sub>A binding to substrate-free enzyme and enzyme-substrate complex, respectively, a likely implication is that Ap<sub>4</sub>A and the first bound substrate molecule mutually stabilize binding of each other to *cp*PPase 20–40-fold.

**Thermodynamics and Stoichiometry of Nucleotide Binding CBS-PPases**—Using ITC allowed the direct measurement of changes in free energy (ΔG), enthalpy (ΔH), and entropic free energy (TΔS) components of nucleotide binding to CBS-PPases. A typical titration profile is shown in Fig. 6A. The results of similar titrations performed with different CBS-PPases and nucleotides are summarized in Fig. 6B and Table 6.

One important result was that titrations of the DRTGG domain-lacking *el*PPase or *mt*PPase with up to 10 μM Ap<sub>4</sub>A or

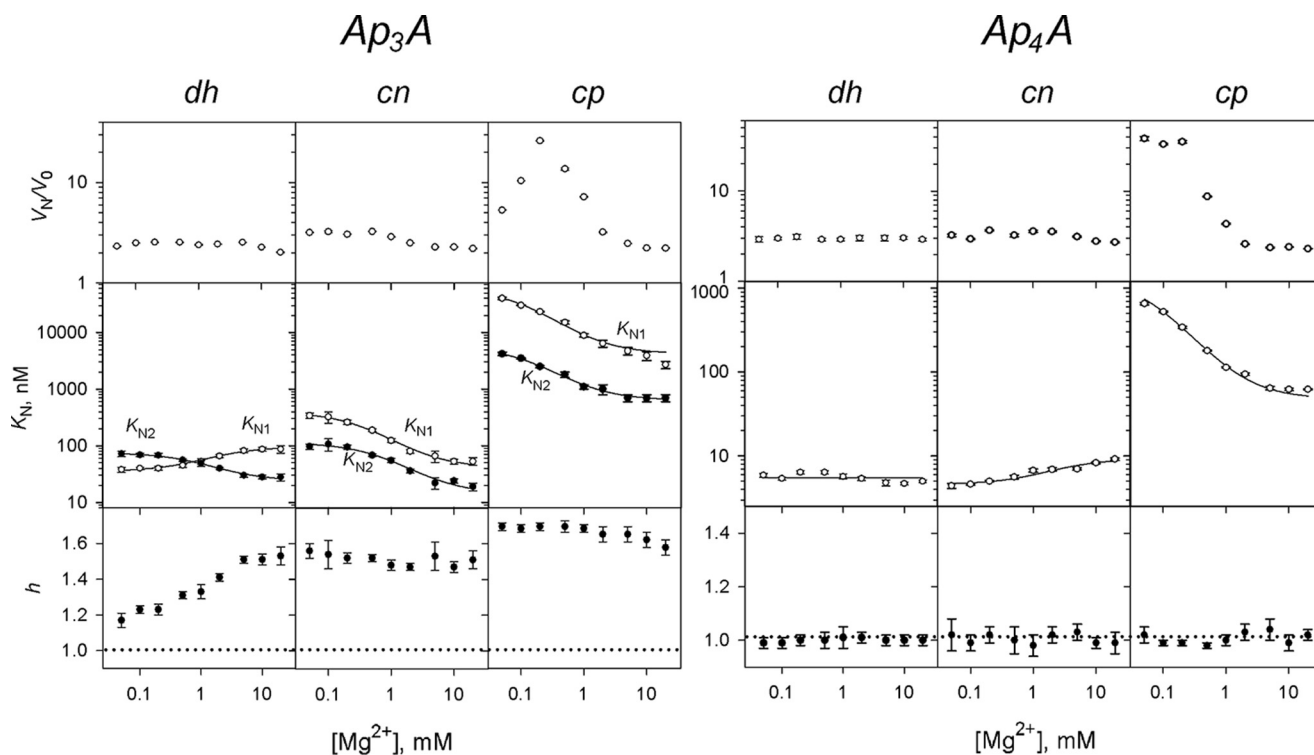


FIGURE 2.  $Mg^{2+}$  concentration dependence of CBS-PPase activation by  $Ap_3A$  (left panel) and  $Ap_4A$  (right panel). The panels show (from top to bottom) the activation factor  $K_{N1}$  (○) and  $K_{N2}$  (●) values and Hill coefficients. The  $K_{N1}$  and  $K_{N2}$  lines show the best fits to Equation 3. The horizontal dotted lines ( $h = 1$ ) mark the boundary between positive and negative cooperativity. *dh*, *dhPPase*; *cn*, *cnPPase*; *cp*, *cpPPase*.

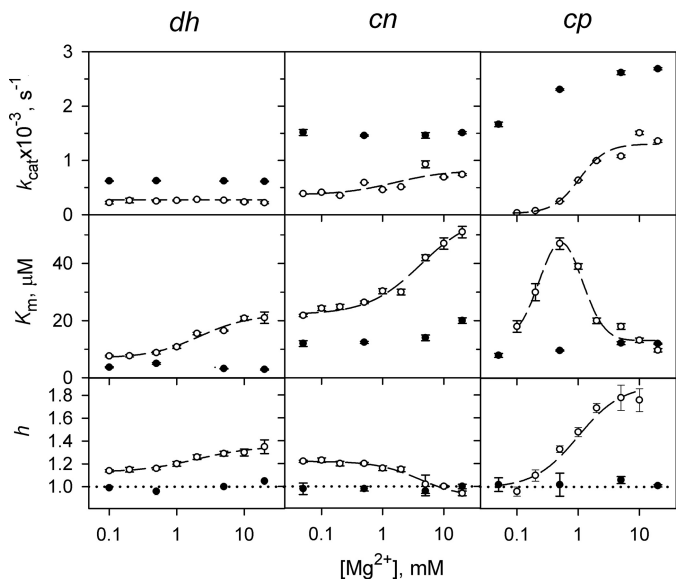


FIGURE 3. **Lack of kinetic cooperativity in CBS-PPases in the presence of  $10 \mu M Ap_4A$ .** The panels show (from top to bottom) the catalytic constant  $k_{cat}$ , the Michaelis constant  $K_m$ , and the Hill coefficient  $h$ . The dashed lines and corresponding points refer to the early estimated parameter values in the absence of  $Ap_4A$  (32);  $K_m$  values refer to the average Michaelis constants ( $\sqrt{K_{m1}K_{m2}}$ ) in this case. The horizontal dotted lines ( $h = 1$ ) mark the boundary between positive and negative cooperativity.  $K_m$  values are measured in terms of the  $MgPP_i$  complex. *dh*, *dhPPase*; *cn*, *cnPPase*; *cp*, *cpPPase*.

$Ap_3A$  produced no ITC signal, consistent with the inability of the dinucleotides to activate these CBS-PPases and modulate their inhibition by ADP. Because the lack of effect on activity did not rule out the possibility of a “silent” binding, the ITC data, which report on a different aspect of the binding reaction,

provided an important support for the lack of complex formation between the DRTGG domain-lacking CBS-PPases and  $Ap_nAs$ . This interpretation was supported by parallel measurements employing AMP, ADP, and ATP (Table 6), which produced similar enthalpy changes in the cases, where previous measurements (32) revealed effects on activity, but no or reduced enthalpy change (*elPPase* with AMP and *cnPPase* with ADP, respectively), where no effect on activity was observed (32). Together, these findings suggest that modulation of activity and heat production are coupled phenomena and that the DRTGG domain is required for tight binding of diadenosine polyphosphates, but not monoadenosine phosphates, to CBS-PPases. The inability of *elPPase* to bind AMP is not associated with the absence of the DRTGG domain because another DRTGG domain-lacking CBS-PPase, *mtPPase*, is inhibited by AMP and hence binds it (31).

Another important finding was that  $\Delta H$ , as calculated per mole of nucleotide, was nearly two times greater for  $Ap_4A$  and  $Ap_5A$  than for  $Ap_3A$  and the mononucleotides in the titrations with the DRTGG domain-containing CBS-PPases. This effect correlated with a 2-fold lower binding stoichiometry for  $Ap_4A$  and  $Ap_5A$  compared with that for mononucleotides and  $Ap_3A$ .

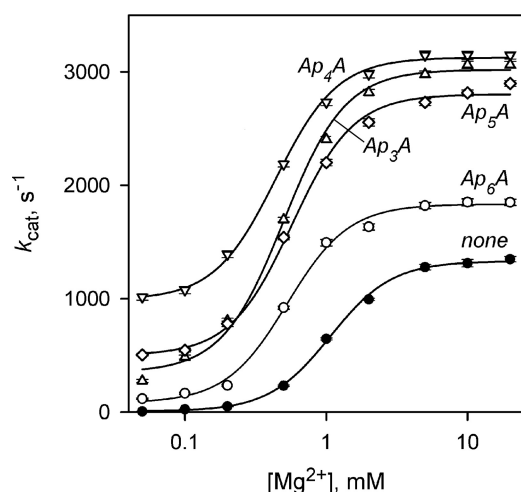
Because of the very tight binding,  $K_N$  and, accordingly,  $T\Delta S$  values could not be estimated with adequate precision in most  $Ap_nA$  titrations. Where  $K_N$  (and hence  $\Delta G$ ) values were available, the free energy change of nucleotide binding was dominated by  $\Delta H$ , with a significant contribution from  $T\Delta S$ , likely because of a hydrophobic effect. The  $K_N$  values derived from ITC measurements are in a fair agreement with those obtained from nucleotide effects on activity (see Ref. 32 for mononucle-

**TABLE 3**Kinetic parameters for nucleotide activation derived from the  $Mg^{2+}$  dependencies of  $K_{N1}$  and  $K_{N2}$  for  $Ap_3A$  or  $K_N$  for  $Ap_4A$  (Fig. 2)

Enzyme	Parameter value									
	$Ap_3A$					$Ap_4A$				
	$K_{N1}$ dependence					$K_{N2}$ dependence				
	$K_{N1,0}$	$K_{N1,M}$	$K_m$	$K_{N2,0}$	$K_{N2,M}$	$K_m$	$K_{N,0}$	$K_{N,M}$	$K_m$	
	<i>HM</i>	<i>HM</i>	<i>HM</i>	<i>HM</i>	<i>HM</i>	<i>HM</i>	<i>HM</i>	<i>HM</i>	<i>HM</i>	
<i>dhPPase</i>	$35 \pm 2$	$96 \pm 3$	$0.7 \pm 0.3$	$75 \pm 2$	$24 \pm 1$	$1.5 \pm 0.4$	$5.5 \pm 0.5$	$5.5 \pm 0.5$	NA <sup>a</sup>	
<i>cnPPase</i>	$390 \pm 10$	$41 \pm 6$	$3.2 \pm 0.7$	$110 \pm 10$	$14 \pm 4$	$5 \pm 3$	$4.3 \pm 0.3$	$8.6 \pm 0.5$	$0.8 \pm 0.3$	
<i>cpPPase</i>	$59,000 \pm 5,000$	$4,200 \pm 700$	$1.4 \pm 0.4$	$5,600 \pm 200$	$640 \pm 50$	$1.1 \pm 0.2$	$1,200 \pm 200$	$55 \pm 3$	$1.4 \pm 0.2$	

<sup>a</sup> NA, not attendant.**TABLE 4**Kinetic parameters for  $PP_i$  hydrolysis in the presence of  $50 \mu M$   $Ap_3A$  and  $5 mM$   $Mg^{2+}$  estimated with Equation 2The values in parentheses refer to parameter values previously measured in the absence of  $Ap_3A$  (32).

Enzyme	$k_{cat}$ $s^{-1}$	$K_{m1}$	$K_{m2}$	$\sqrt{K_{m1}K_{m2}}$	$4K_{m1}/K_{m2}$	$h$
<i>dhPPase</i>	$565 \pm 4$ (350)	$1.47 \pm 0.03$ (26)	$5.8 \pm 0.3$ (10)	$2.9 \pm 0.1$ (20)	$1.01 \pm 0.07$	$1.00 \pm 0.02$ (1.29)
<i>cnPPase</i>	$1,120 \pm 20$ (540)	$5.0 \pm 0.4$ (23)	$18 \pm 3$ (80)	$9.5 \pm 0.6$ (44)	$1.1 \pm 0.2$	$1.02 \pm 0.04$ (1.02)
<i>cpPPase</i>	$3,090 \pm 20$ (1,080)	$13 \pm 1$ (80)	$16 \pm 1$ (4)	$14.5 \pm 0.4$ (18)	$3.2 \pm 0.3$	$1.23 \pm 0.02$ (1.8)

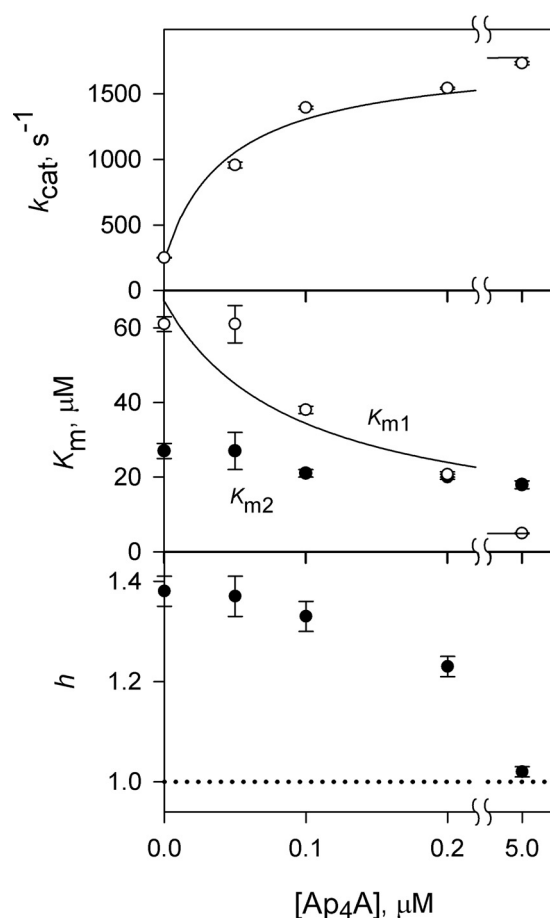
**FIGURE 4.**  $Mg^{2+}$  concentration dependence of  $k_{cat}$  for *cpPPase* measured in the presence of  $50 \mu M$   $Ap_3A$  or  $10 \mu M$   $Ap_4A$  or  $Ap_5A$ . The values of  $k_{cat}$  were fit to the equation  $k_{cat} = k_{cat,0} + (k_{cat,M} - k_{cat,0}) / (1 + (K_m/[M])^2)$ , where  $k_{cat,0}$  and  $k_{cat,M}$  are the limiting values of  $k_{cat}$  at 0 and infinite  $Mg^{2+}$  concentrations, respectively, and  $K_m$  is the metal binding constant.**TABLE 5**Kinetic parameters describing effects of  $Mg^{2+}$  on  $k_{cat}$  for *cpPPase* in the presence of diadenosine polyphosphates

$Ap_nA$	$k_{cat,0}$ $s^{-1}$	$k_{cat,m}$ $s^{-1}$	$K_m$ <i>HM</i>
None	$6 \pm 13$	$1,330 \pm 20$	$1.07 \pm 0.03$
$Ap_3A$ ( $50 \mu M$ )	$350 \pm 50$	$3,020 \pm 40$	$0.50 \pm 0.03$
$Ap_4A$ ( $10 \mu M$ )	$990 \pm 30$	$3,130 \pm 20$	$0.44 \pm 0.02$
$Ap_5A$ ( $10 \mu M$ )	$500 \pm 40$	$2,800 \pm 30$	$0.57 \pm 0.03$
$Ap_6A$ ( $10 \mu M$ )	$80 \pm 30$	$1,830 \pm 30$	$0.53 \pm 0.03$

otides and Table 1 for  $Ap_3A$ ). It should be noted that ITC measurements can hardly distinguish positive binding cooperativity and yield an average  $\Delta H$  value for all binding sites.

## Discussion

CBS domains, found in many proteins, are known for their ability to bind adenine nucleotides and in this way regulate activities of their carrier proteins. The list of regulating adenine nucleotides includes AMP, ADP, ATP, *S*-adenosyl methionine, NADH, and analogs of AMP and ATP (27). Examples of less

**FIGURE 5.**  $Ap_4A$  concentration dependence of kinetic cooperativity in *cpPPase* in the presence of  $0.5 mM$   $Mg^{2+}$ . Notations are as in Fig. 4. The values of  $k_{cat}$  were fit to the equation  $k_{cat} = k_{cat,0} + (k_{cat,N} - k_{cat,0}) / (1 + K_N/[M])$ , where  $k_{cat,0}$  and  $k_{cat,M}$  are the limiting values of  $k_{cat}$  at 0 and infinite  $Ap_4A$  concentrations, respectively, and  $K_N$  is the nucleotide binding constant. The line for  $K_{m1}$  shows the best fit to Equation 3.

common CBS domain ligands include  $Mg^{2+}$  (38), DNA, and RNA (39, 40). We earlier reported that crystals of the isolated dimeric regulatory region of *cpPPase* grown in the presence of  $Ap_4A$  contains one  $Ap_4A$  molecule per dimer bridging two

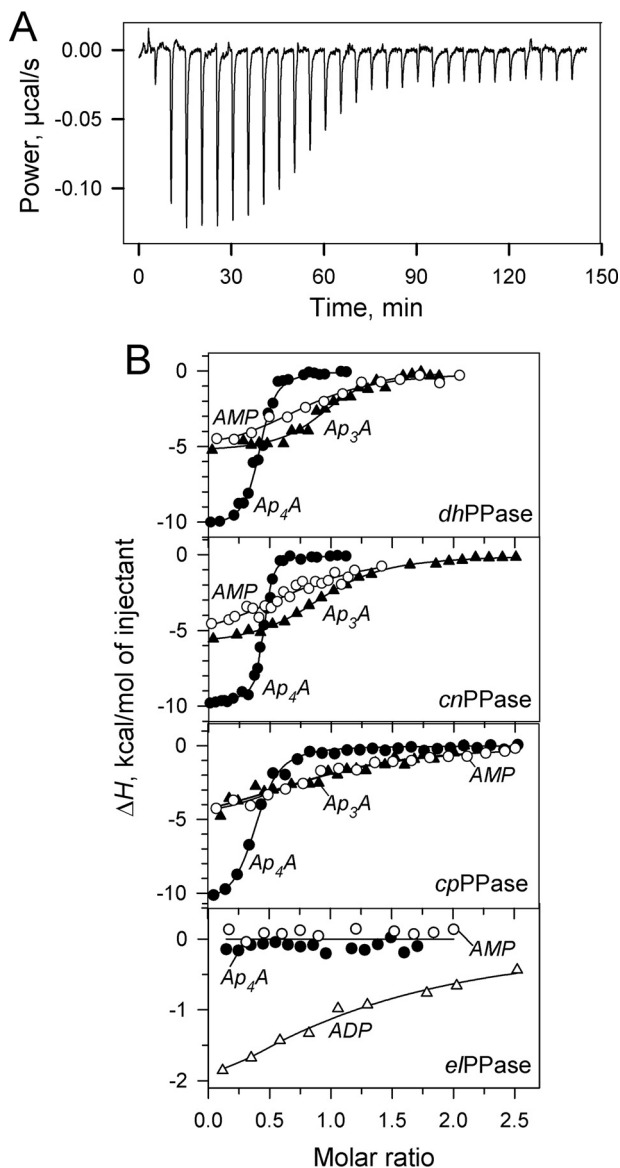


FIGURE 6. ITC measurements of nucleotide binding to CBS-PPases. *A*, typical raw data for successive injections of  $Ap_4A$  into  $dhPPase$  solution. *B*, integrated heats for titration of four CBS-PPases by selected mono- and dinucleotides after correction for dilution. Enzyme dimer concentration was  $4 \mu M$  ( $dhPPase$ ),  $5 \mu M$  ( $cnPPase$ ),  $3.5 \mu M$  ( $cpPPase$ ), or  $2.5 \mu M$  ( $elPPase$ ). The lines show the best fits for a single-binding site model.

pairs of CBS domains, whereas each CBS domain pair binds an AMP molecule (33). We also found that  $Ap_4A$  induces a significant opening of the interface compared with the AMP-bound form. The results reported above extend these earlier findings by showing that (a)  $Ap_nAs$  with  $n = 3-6$  bind three CBS-PPases with nanomolar affinity and activate them *in vitro*; (b)  $Ap_nA$  binding is only observed in CBS-PPases that have an intercalating DRTGG domain in the regulatory region; and (c) unlike common adenine nucleotides, long chain  $Ap_nAs$  ( $n > 3$ ) abolish or markedly reduce kinetic cooperativity (non-Michaelian behavior) in CBS-PPases. The unique features of  $Ap_nA$  complexes of CBS-PPases compared with those of their complexes with mononucleotides and complexes of other CBS proteins with their regulating ligands are described below. Notably,

TABLE 6  
Thermodynamic parameters for nucleotide complexes of CBS-PPases obtained by isothermal calorimetry

Enzyme/nucleotide	$K_N$ $\mu M$	$n$	$\Delta H$ kcal/mol	$-T\Delta S$ kcal/mol
<i>dhPPase</i>				
AMP	$0.8 \pm 0.3$	$0.79 \pm 0.05$	$-5.6 \pm 0.5$	$-2.7 \pm 0.6$
ADP	$1.0 \pm 0.2$	$0.85 \pm 0.04$	$-5.9 \pm 0.4$	$-2.4 \pm 0.5$
ATP	$1.2 \pm 0.1$	$0.80 \pm 0.02$	$-5.8 \pm 0.2$	$-2.4 \pm 0.2$
$Ap_3A$	$0.12 \pm 0.05$	$0.97 \pm 0.02$	$-5.3 \pm 0.2$	$-4.0 \pm 0.3$
$Ap_4A$		$0.41 \pm 0.01$	$-10.4 \pm 0.3$	
$Ap_5A$		$0.41 \pm 0.01$	$-10.3 \pm 0.3$	
<i>cnPPase</i>				
AMP	$0.9 \pm 0.4$	$0.80 \pm 0.08$	$-5.9 \pm 0.9$	$-2.4 \pm 1.0$
ADP	$5 \pm 1$	$0.91 \pm 0.08$	$-3.0 \pm 0.6$	$-4.1 \pm 1.0$
ATP	$0.6 \pm 0.2$	$0.89 \pm 0.07$	$-5.8 \pm 0.7$	$-2.8 \pm 1.1$
$Ap_3A$		$0.94 \pm 0.01$	$-6.1 \pm 0.1$	
$Ap_4A$		$0.44 \pm 0.01$	$-9.7 \pm 0.3$	
<i>cpPPase</i>				
AMP	$0.97 \pm 0.03$	$0.87 \pm 0.06$	$-6.0 \pm 0.6$	$-2.3 \pm 0.7$
ADP	$2.6 \pm 0.5$	$0.94 \pm 0.09$	$-6.0 \pm 0.8$	$-1.6 \pm 0.3$
ATP	$0.23 \pm 0.06$	$1.00 \pm 0.03$	$-5.6 \pm 0.3$	$-3.6 \pm 0.9$
$Ap_3A$	$0.7 \pm 0.3$	$0.97 \pm 0.11$	$-5.7 \pm 1.1$	$-2.7 \pm 1.2$
$Ap_4A$		$0.42 \pm 0.01$	$-10.4 \pm 0.3$	
<i>elPPase</i>				
AMP			$\leq 0.1$	
ADP	$9 \pm 4$	$0.95 \pm 0.1$	$-4.5 \pm 1.6$	$-2.4 \pm 2.0$
ATP	$5 \pm 1$	$1.0 \pm 0.4$	$-8 \pm 4$	$-0.5 \pm 0.3$
$Ap_3A$			$\leq 0.1$	
$Ap_4A$			$\leq 0.1$	

$Ap_nAs$  have not been reported as ligands for any other CBS protein.

Based on their binding properties,  $Ap_nAs$  can be divided into two groups.  $Ap_3A$  bound to CBS-PPases cooperatively and with lower affinity, as characterized by either  $K_{N1}$  and  $K_{N2}$  or their average value ( $\sqrt{K_{N1}K_{N2}}$ ) (Table 1). The other dinucleotides ( $n = 4-6$ ) bound noncooperatively and with a higher affinity that did not depend significantly on the  $n$  value (Table 2). The affinities of  $Ap_nAs$  with  $n = 4-6$  for CBS-PPases surpassed that of adenine mononucleotides (32) by 2-3 orders of magnitude. Such high affinities are unprecedented among other CBS proteins, which generally bind their nucleotide ligands in the millimolar range. The difference in the binding affinities of the two  $Ap_nA$  groups was most pronounced with  $cpPPase$ , amounting to 3 orders of magnitude. As previously demonstrated (33),  $Ap_4A$  interacts through both of its adenine moieties with two CBS domain pairs of different subunits in  $cpPPase$ . Such an arrangement is also likely with  $Ap_5A$  and  $Ap_6A$ , consistent with their similar  $\Delta H$  values and binding stoichiometries, determined from ITC measurements (Table 6). In contrast,  $\Delta H$  for  $Ap_3A$  was half that of  $Ap_5A$  and  $Ap_6A$ , and the binding stoichiometry was 2-fold higher, similar to values for mononucleotides (Table 6). These observations likely indicate that  $Ap_3A$  predominantly binds CBS-PPases through only one adenine moiety.

The binding affinities of  $Ap_nAs$  showed a complex dependence on substrate and metal cofactor concentrations. At a constant  $Mg^{2+}$  concentration, substrate increased the binding affinities of  $dhPPase$  and  $cpPPase$  for all  $Ap_nAs$  but exerted an opposite effect on  $cnPPase$  (Tables 1 and 2). Accordingly,  $Ap_3A$  (Table 4) and  $Ap_4A$  (Fig. 3) decreased the average Michaelis constant ( $\sqrt{K_{m1}K_{m2}}$  and  $K_m$ ). The effect of  $Ap_3A$  on  $\sqrt{K_{m1}K_{m2}}$  for  $cpPPase$  measured in the presence of  $5 \text{ mM } Mg^{2+}$  was quite modest, but keeping in mind the bell-shaped dependence of  $\sqrt{K_{m1}K_{m2}}$  on  $[Mg^{2+}]$  for this enzyme in the absence of adenine

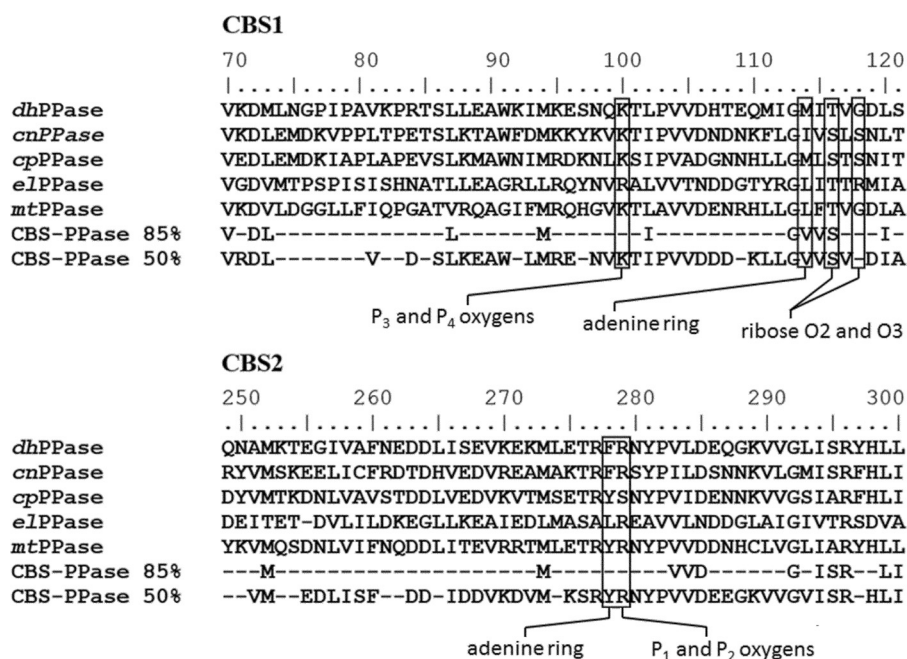


FIGURE 7. **Aligned amino acid sequences of the two CBS domains of the characterized CBS-PPases.** Amino acid residues making contacts with  $Ap_4A$  or AMP in the crystal structures of  $cpPPase$  (33) are shown in boxes. Consensus residues based on 180 CBS-PPase sequences are indicated in the two bottom lines. Residue numbering is for full-length  $cpPPase$ . Consensus residues for different levels of identity are indicated below the set of sequences.

nucleotides (Fig. 3), one would expect, by analogy, greater effects of  $Ap_3A$  at low  $[Mg^{2+}]$ .

However, the most striking effect of  $Ap_nAs$  on substrate binding was abolition of kinetic cooperativity. This effect was observed with both  $Ap_3A$  and  $Ap_4A$ , representing the two dinucleotide groups and might be explained by two different mechanisms. First, the effectors may disrupt the communication between active sites, allowing them to function independently. Alternatively, the dinucleotides may induce asymmetry in the enzyme dimer such that only one active site operates in the dimer (ultimate negative cooperativity). Determining the three-dimensional structure of the enzyme with bound dinucleotide would make it possible to discriminate between these alternative explanations.

$Mg^{2+}$  effects on nucleotide binding also varied depending on the enzyme (Fig. 2) and differed from those observed with adenine mononucleotides (32). With  $Ap_3A$ , values of  $K_{N1}$  and  $K_{N2}$  for  $dhPPase$  changed in different directions, decreasing the degree of cooperativity at low  $[Mg^{2+}]$  (Fig. 2A). No bound  $Mg^{2+}$  ion was observed in the structure of the regulatory region of  $cpPPase$  (33), suggesting that the modulatory  $Mg^{2+}$  resides in the active site. Notable in this regard, three  $Mg^{2+}$  ions per active site participate in catalysis among homologous nonregulated family II PPases (24, 41). The effects of  $Mg^{2+}$  on nucleotide binding may, in part, be a consequence of its effects on substrate binding, because these measurements were carried out at a nonsaturating substrate concentration (50  $\mu M$ ).

Both  $Ap_3A$  and  $Ap_4A$  activated CBS-PPases under the conditions tested because of favorable changes in both  $k_{cat}$  and the average Michaelis constant ( $\sqrt{K_{m1}K_{m2}}$ ) (Table 4 and Fig. 3). Accordingly, the degree of activation was greater at low substrate concentrations (Table 1) and varied from severalfold to several ten-fold. The largest effects were observed with

$cpPPase$ . Based on its  $k_{cat}$  and  $K_m$  values (Fig. 3), this enzyme is predicted to be activated by  $Ap_4A$  in the presence of 1 mM  $Mg^{2+}$  by a factor of  $\sim 51$  and  $\sim 19$  at substrate concentrations of 1 and 10  $\mu M$ , respectively. At low  $[Mg^{2+}]$ , the activating effect of  $Ap_nA$  is dominated by  $k_{cat}$ , especially with  $cpPPase$  (Fig. 4 and Table 5). In this enzyme,  $k_{cat}$  is strongly  $Mg^{2+}$ -dependent and  $Ap_nA$  markedly released this dependence by allowing catalysis in the enzyme with a vacant  $Mg^{2+}$  site and by somewhat increasing its affinity for  $Mg^{2+}$  (Table 5). In this respect,  $Ap_nAs$  partially substitute for  $Mg^{2+}$  as an enzyme activator.

Qualitatively similar activating effects on CBS-PPases were previously observed with ATP (31, 32), although ATP effects were smaller in size and required much higher effector concentrations. A further difference is that ATP bound cooperatively, like  $Ap_3A$ . The effects of ATP and  $Ap_3A$  are thus similar in many aspects. As noted above, activator binding induces significant opening of the CBS domain interface (33). Such opening can be achieved upon binding of a single molecule of  $Ap_4A$  or a longer dinucleotide that binds to both subunits of CBS-PPase through two adenine moieties. Structure modeling of the  $cpPPase$  regulatory region indicated that the polyphosphate chain of  $Ap_3A$  is too short for this binding mode. In this case, and with ATP, interface opening apparently results from repulsion between two molecules of the effector bound to different subunits.

The requirement for an intercalating DRTGG domain for  $Ap_nA$  binding to CBS domains provides another interpretive challenge. In the structure of the regulatory region and the modeled structure of the whole  $cpPPase$ , both the DRTGG domain and CBS domain pairs participate in forming the subunit interface (33). DRTGG domain-containing CBS-PPases apparently have a larger binding cavity for the regulating ligands or increased flexibility of the CBS domains at the



## Nucleotide-regulated Soluble Pyrophosphatases

expense of their smaller contribution to the subunit contact area, allowing them to accommodate more bulky  $Ap_nA$  molecules. This interpretation is supported by data showing that the DRTGG domain-deficient *el*PPase (32) and *mt*PPase (31) bind ATP with an affinity 1–2 orders of magnitude lower than that of the less bulky AMP and ADP. In contrast, no such discrimination is observed in DRTGG domain-containing CBS-PPases (32). Notably, the primary structures of the CBS domains in DRTGG domain-deficient CBS-PPases (Fig. 7) do not contain specific mutations that would disallow their binding of  $Ap_nAs$ . Despite a generally low degree of residue conservation in CBS domains, all residues involved in nucleotide binding are found in at least one of the DRTGG domain-deficient CBS-PPases. Based on these considerations,  $Ap_nAs$  are not expected to bind with comparable affinity to the numerous other CBS proteins that lack a DRTGG or other intercalating domain.

$Ap_nA$  binding is expected to significantly change CBS-PPase activity *in vivo*, particularly under low energy conditions, when the concentration of the alternative activator, ATP, is low. Although basal intracellular levels of  $Ap_nAs$  are 4 orders of magnitude lower than those of adenine mononucleotides,  $Ap_nA$  concentrations can rise by 2 orders of magnitude under stress conditions (42, 43). Also taking into consideration their extraordinarily high affinity,  $Ap_nAs$  could be expected to efficiently compete with mononucleotides for CBS-PPase binding in these circumstances. An increase in CBS-PPase activity is expected to decrease the concentration of  $PP_i$  and thus release  $PP_i$ -mediated inhibition of numerous biosynthetic reactions in which  $PP_i$  is produced as a by-product (44). That the affinity of CBS-PPases for  $Ap_nAs$  markedly surpasses that of all known  $Ap_nA$ -binding proteins suggests that this enzyme is a dominant target through which  $Ap_nAs$  fulfill their stress response-related functions in bacteria.

**Author Contributions**—V. A. A. designed, performed and analyzed the experiments, and contributed to writing the manuscript. A. S. designed and constructed vectors, expressed and purified proteins, and performed bioinformatics analyses. H. K. T. performed ITC experiments with dhPPase. V. N. O. supervised ITC experiments and data analysis. R. L. designed and supervised the experiments. A. A. B. designed and analyzed experiments and wrote the manuscript. All authors reviewed the results and approved the final version of the manuscript.

**Acknowledgment**—We thank Dr. P. Semenyuk for help with ITC measurements.

### References

1. Reiss, J. R., and Moffatt, J. G. (1965) Dismutation reactions of nucleoside polyphosphates. III. the synthesis of  $\alpha,\omega$ -dinucleoside 5'-polyphosphates. *J. Org. Chem.* **30**, 3381–3387
2. Fraga, H., and Fontes, R. (2011) Enzymatic synthesis of mono and dinucleoside polyphosphates. *Biochim. Biophys. Acta* **1810**, 1195–1204
3. Zamecnik, P. C., Stephenson, M. L., Janeway, C. M., and Randerath, K. (1966) Enzymatic synthesis of diadenosine tetraphosphate and diadenosine triphosphate with a purified lysyl-sRNA synthetase. *Biochem. Biophys. Res. Commun.* **24**, 91–97
4. Goerlich, O., Foeckler, R., and Holler, E. (1982) Mechanism of synthesis of adenosine(5')tetraphospho(5')adenosine (AppppA) by aminoacyl-tRNA synthetases. *Eur. J. Biochem.* **126**, 135–142
5. Wright, M., Boonyalai, N., Tanner, J. A., Hindley, A. D., and Miller, A. D. (2006) The duality of LysU, a catalyst for both  $Ap_4A$  and  $Ap_3A$  formation. *FEBS J.* **273**, 3534–3544
6. Guranowski, A. (2000) Specific and nonspecific enzymes involved in the catabolism of mononucleoside and dinucleoside polyphosphates. *Pharmacol. Ther.* **87**, 117–139
7. Jiang, Y.-L., Zhang, J.-W., Yu, W.-L., Cheng, W., Zhang, C.-C., Flolet, C., Di Guilmi, A.-M., Vernet, T., Zhou, C.-Z., and Chen, Y. (2011) Structural and enzymatic characterization of the streptococcal ATP/diadenosine polyphosphate and phosphodiester hydrolase Spr1479/SapH. *J. Biol. Chem.* **286**, 35906–35914
8. Lee, P. C., Bochner, B. R., and Ames, B. N. (1983) AppppA, heat shock stress, and cell oxidation. *Proc. Natl. Acad. Sci. U.S.A.* **80**, 7496–7500
9. Bochner, B. R., Zyllicz, M., and Georgopoulos, C. (1986) *Escherichia coli* DnaK protein possesses a 5'-nucleotidase activity that is inhibited by AppppA. *J. Bacteriol.* **168**, 931–935
10. Varshavsky, A. (1983) Diadenosine 5',5''-P<sup>1</sup>,P<sup>4</sup>-tetraphosphate: a pleiotypically acting alarmone. *Cell* **34**, 711–712
11. Tanner, J. A., Wright, M., Christie, E. M., Preuss, M. K., and Miller, A. D. (2006) Investigation into the interactions between diadenosine 5',5''-P<sup>1</sup>,P<sup>4</sup>-tetraphosphate and two proteins: molecular chaperone GroEL and cAMP receptor protein. *Biochemistry* **45**, 3095–3106
12. Tshori, S., Razin, E., and Nechushtan, H. (2013) Amino-acyl tRNA synthetases generate dinucleotide polyphosphates as second messengers: functional implications. *Top. Curr. Chem.* **344**, 10–12
13. Sillero, M. A., De Diego, A., Osorio, H., and Sillero, A. (2002) Dinucleoside polyphosphates stimulate the primer independent synthesis of poly(A) catalyzed by yeast poly(A) polymerase. *Eur. J. Biochem.* **269**, 5323–5329
14. Nishimura, A., Moriya, S., Ukai, H., Nagai, K., Wachi, M., and Yamada, Y. (1997) Diadenosine 5',5''-P<sup>1</sup>,P<sup>4</sup>-tetraphosphate (Ap<sub>4</sub>A) controls the timing of cell division in *Escherichia coli*. *Genes Cells* **2**, 401–413
15. Gómez-Villafuertes, R., Pintor, J., Gualix, J., and Miras-Portugal, M. T. (2004) GABA modulates presynaptic signalling mediated by dinucleotides on rat synaptic terminals. *J. Pharmacol. Exp. Ther.* **308**, 1148–1157
16. Vartanian, A. A., Suzuki, H., and Poletaev, A. I. (2003) The involvement of diadenosine 5',5''-P<sup>1</sup>,P<sup>4</sup>-tetraphosphate in cell cycle arrest and regulation of apoptosis. *Biochem. Pharmacol.* **65**, 227–235
17. Giraldez, L., Díaz-Hernández, M., Gómez-Villafuertes, R., Pintor, J., Castro, E., and Miras-Portugal, M. T. (2001) Adenosine triphosphate and diadenosine pentaphosphate induce  $[Ca^{2+}]_i$  increase in rat basal ganglia aminergic terminals. *J. Neurosci. Res.* **64**, 174–182
18. Conant, A. R., Theologou, T., Dihmis, W. C., and Simpson, A. W. (2008) Diadenosine polyphosphates are selective vasoconstrictors in human coronary artery bypass grafts cells. *Vascul. Pharmacol.* **48**, 157–164
19. Johnstone, D. B., and Farr, S. B. (1991) AppppA binds to several proteins in *Escherichia coli*, including the heat shock and oxidative stress proteins DnaK, GroEL, E89, C45 and C40. *EMBO J.* **10**, 3897–3904
20. Guo, W., Azhar, M. A., Xu, Y., Wright, M., Kamal, A., and Miller, A. D. (2011) Isolation and identification of diadenosine 5',5''-P<sup>1</sup>,P<sup>4</sup>-tetraphosphate binding proteins using magnetic bio-panning. *Bioorg. Med. Chem. Lett.* **21**, 7175–7179
21. Azhar, M. A., Wright, M., Kamal, A., Nagy, J., and Miller, A. D. (2014) Biotin-c10-AppCH2ppA is an effective new chemical proteomics probe for diadenosine polyphosphate binding proteins. *Bioorg. Med. Chem. Lett.* **24**, 2928–2933
22. Marques, A. F., Teixeira, N. A., Gambaretto, C., Sillero, A., and Sillero M. A. (1998) IMP-GMP 5'-nucleotidase from rat brain: activation by polyphosphates. *J. Neurochem.* **71**, 1241–1250
23. Kajander, T., Kellosalo, J., and Goldman, A. (2013) Inorganic pyrophosphatases: one substrate, three mechanisms. *FEBS Lett.* **587**, 1863–1869
24. Parfenyev, A. N., Salminen, A., Halonen, P., Hachimori, A., Baykov, A. A., and Lahti, R. (2001) Quaternary structure and metal-ion requirement of family II pyrophosphatases from *Bacillus subtilis*, *Streptococcus gordonii* and *Streptococcus mutans*. *J. Biol. Chem.* **276**, 24511–24518
25. Bateman, A. (1997) The structure of a domain common to archaeobacteria and the homocystinuria disease protein. *Trends Biochem. Sci.* **22**, 12–13
26. Ereño-Orbea, J., Oyenarte, I., and Martínez-Cruz, L. A. (2013) CBS domains: ligand binding sites and conformational variability. *Arch. Biochem.*

- Biophys.* **540**, 70–81
27. Baykov A. A., Tuominen H. K., and Lahti R. (2011) The CBS domain: a protein module with an emerging prominent role in regulation. *ACS Chem. Biol.* **6**, 1156–1163
  28. Kemp, B. E. (2004) Bateman domains and adenosine derivatives form a binding contract. *J. Clin. Invest.* **113**, 182–184
  29. Ignoul, S., and Eggermont, J. (2005) CBS domains: structure, function, and pathology in human proteins. *Am. J. Physiol. Cell Physiol.* **289**, C1369–C1378
  30. Scott, J. W., Hawley, S. A., Green, K. A., Anis, M., Stewart, G., Scullion, G. A., Norman, D. G., and Hardie, D. G. (2004) CBS domains form energy-sensing modules whose binding of adenosine ligands is disrupted by disease mutations. *J. Clin. Invest.* **113**, 274–284
  31. Jämsen, J., Tuominen, H., Salminen, A., Belogurov, G. A., Magretova, N. N., Baykov, A. A., and Lahti, R. (2007) A CBS domain-containing pyrophosphatase of *Moorella thermoacetica* is regulated by adenine nucleotides. *Biochem. J.* **408**, 327–333
  32. Salminen A., Anashkin V. A., Lahti M., Tuominen H. K., Lahti R., Baykov A. A. (2014) Cystathionine  $\beta$ -synthase (CBS) domains confer multiple forms of  $Mg^{2+}$ -dependent cooperativity to family II pyrophosphatases. *J. Biol. Chem.* **289**, 22865–22876
  33. Tuominen, H., Salminen, A., Oksanen, E., Jämsen, J., Heikkilä, O., Lehtiö, L., Magretova, N. N., Goldman, A., Baykov, A. A., and Lahti, R. (2010) Crystal structures of the CBS and DRTGG domains of the regulatory region of *Clostridium perfringens* pyrophosphatase complexed with the inhibitor, AMP, and activator, diadenosine tetraphosphate. *J. Mol. Biol.* **398**, 400–413
  34. Jämsen, J., Baykov, A. A., and Lahti, R. (2012) Fast kinetics of nucleotide binding to *Clostridium perfringens* family II pyrophosphatase containing CBS and DRTGG domains *Biochemistry* **77**, 165–170
  35. Baykov, A. A., and Awaeva, S. M. (1981) A simple and sensitive apparatus for continuous monitoring of orthophosphate in the presence of acid-labile compounds. *Anal. Biochem.* **116**, 1–4
  36. Baykov, A. A., Bakuleva, N. P., and Rea, P. A. (1993) Steady-state kinetics of substrate hydrolysis by vacuolar  $H^+$ -pyrophosphatase. A simple three-state model. *Eur. J. Biochem.* **217**, 755–762
  37. Bisswanger, H. (2008) *Enzyme Kinetics: Principles and Methods*, 2nd Ed., pp. 14–17, Wiley-VCH Verlag, Weinheim, Germany
  38. Hattori, M., Tanaka, Y., Fukai, S., Ishitani, R., and Nureki, O. (2007) Crystal structure of the MgtE  $Mg^{2+}$  transporter. *Nature* **448**, 1072–1075
  39. McLean, J. E., Hamaguchi, N., Belenky, P., Mortimer, S. E., Stanton, M., and Hedstrom, L. (2004) Inosine 5'-monophosphate dehydrogenase binds nucleic acids *in vitro* and *in vivo*. *Biochem. J.* **379**, 243–251
  40. Aguado-Llera, D., Oyenarte, I., Martínez-Cruz, L. A., and Neira, J. L. (2010) The CBS domain protein MJ0729 of *M. jannaschii* binds DNA. *FEBS Lett.* **584**, 4485–4489
  41. Fabrichniy, I. P., Lehtiö, L., Tammenkoski, M., Zyryanov, A. B., Oksanen, E., Baykov, A. A., Lahti, R., and Goldman, A. (2007) A trimetal site and ground-state substrate distortion mark the active site of family II inorganic pyrophosphatase. *J. Biol. Chem.* **282**, 1422–1431
  42. Garrison, P. N., and Barnes, L. D. (1992) Determination of dinucleoside polyphosphates, in *Ap<sub>4</sub>A and Other Dinucleoside Polyphosphates* (McLennan, A.G., ed) pp. 29–61, CRC Press, Boca Raton, FL
  43. Plateau, P., and Blanquet, S. (1994) Dinucleoside oligophosphates in micro-organisms. *Adv. Microb. Physiol.* **36**, 81–109
  44. Heinonen, J. K. (2001) *Biological Role of Inorganic Pyrophosphate*, pp. 123–188, Kluwer Academic Publishers, London